PRP Pharmacology Research & Perspectives
Open Access

ORIGINAL ARTICLE

Use of a novel rapid and resource-efficient cassette dosing approach to determine the pharmacokinetics and CNS distribution of small molecule 7-transmembrane receptor allosteric modulators in rat

Thomas. M. Bridges, Ryan D. Morrison, Frank W. Byers, Shuanghui Luo & J. Scott Daniels

Drug Metabolism and Pharmacokinetics, Vanderbilt Center for Neuroscience Drug Discovery, Vanderbilt University Medical Center, Nashville, Tennessee, 37232

Keywords
Cassette, pharmacokinetics, allosteric modulator, distribution

Correspondence
J. Scott Daniels, Drug Metabolism & Pharmacokinetics, Vanderbilt Center for Neuroscience Drug Discovery, Vanderbilt University Medical Center, Nashville, TN 37232. Tel: 615-322-0673; Fax: 615-875-3375; E-mail: scott.daniels@vanderbilt.edu

Funding Information
Portions of this work were funded by AstraZeneca (Neuroscience Innovative Medicines) and the National Institutes of Health (U54MH084659; U01MH087965).

Received: 4 April 2014; Revised: 17 June 2014; Accepted: 21 June 2014

Pharma Res Per, 2(6), 2014, e00077, doi: 10.1002/prp2.77

doi: 10.1002/prp2.77

Abstract

Approaches to efficiently and accurately define the pharmacokinetics (PK) of large sets of small molecules in rodents have been previously described. Likewise, a variety of methods for determining brain tissue distribution (BTD) have been reported for use in the discovery of therapeutics targeting the central nervous system (CNS). Herein we describe a novel cassette approach to efficiently obtain concurrent PK and BTD data from a dose of up to five compounds in one rat over 24 h. In conjunction with fraction unbound (f_u) data obtained in plasma and brain homogenate, this approach serves as an efficient means to determine compound unbound brain:unbound plasma partition coefficients ($K_{p,uu}$), thereby providing insight to compounds bearing poor permeability and/or active transporter activity impacting their permeation of the blood–brain barrier (BBB). This integrated approach was utilized in a lead optimization effort towards the discovery of CNS-penetrant allosteric modulators of a seven-transmembrane (7TM) receptor target. Rat PK and brain distribution was rapidly obtained for 70 compounds and correlated to data obtained from in vitro assessments. Two compounds that were evaluated in cassette and discrete studies, displayed agreement in PK (compound 1: cassette CL_p = 1.6 mL min^{-1} kg^{-1}, discrete CL_p = 1.6 mL min^{-1} kg^{-1}; compound 2: cassette CL_p = 11 mL min^{-1} kg^{-1}, discrete CL_p = 8.1 mL min^{-1} kg^{-1}) and BTD (compound 1: cassette K_p = 0.11, discrete K_p = 0.09; compound 2: cassette K_p < 0.05, discrete K_p = 0.04). The resulting data were used to guide medicinal chemistry efforts and to enable the progression of optimized compounds to in vivo pharmacodynamic assessments.

Abbreviations

7TM, seven-transmembrane; AUC, area under the curve; BBB, blood–brain barrier; BHB, brain homogenate binding; BTD, brain tissue distribution; CL_p, plasma clearance; CNS, central nervous system; CSF, cerebrospinal fluid; ER, efflux ratio; f_u, fraction unbound; IP, intraperitoneal; IV, intravenous; IVIVC, in vitro:in vivo correlation; $K_{p,uu}$, unbound distribution partition coefficient; K_p, distribution partition coefficient; LC/MS/MS, liquid chromatography-mass spectrometry; MDCK, Madin-Darby Canine Kidney; P_{app}, apparent permeability; Pgp, P-glycoprotein; PK, pharmacokinetics; PO, per os or oral; PPB, plasma protein binding; SAR, structure-activity relationship; WT, wild type.

Introduction

Pharmacokinetic (PK) studies in rodent species (e.g., Sprague–Dawley [SD] rat) employing intravenous (IV) administration of small molecule test compounds represent a cornerstone of contemporary drug discovery programs as rodent PK data are often used to rank-order compounds based on plasma clearance (CL_p), to establish critical structure-activity relationships (SAR) useful for guiding medicinal chemistry efforts, and to gauge the predicted human PK using one or more allometry approaches (Mahmood and Balian 1996; Goteti et al. 2008; Hosea et al. 2009). Concurrent IV administration of low doses (e.g., 0.1–0.2 mg kg^{-1}) of multiple compounds (e.g., 5–10) via cassettes formulated directly from dimethyl sulfoxide (DMSO) stock solutions (10 mmol L^{-1}) is now a widely adopted practice (Christ 2001; White and Manitpisitkul 2001; Zhang et al. 2004; Smith et al. 2007) and one which enables efficient and accurate determination of pertinent time-concentration parameters valuable for the prediction of human PK; compare to conventional low-throughput discrete PK assessment in which a single compound is administered to multiple animals at fivefold higher doses (typically prepared from solid material). Moreover, cassette dosing employing serial blood sampling from a single animal, together with liquid chromatography-mass spectrometry (LC/MS/MS) bioanalysis using standard curves conveniently prepared as a combination of compounds from DMSO stocks, has become increasingly common due to the efficiency and accuracy of contemporary electrospray ionization mass spectrometric analysis (Huang et al. 2004; Sadagopan et al. 2005; Bueters et al. 2011; Chen et al. 2012).

In the case of neurotherapeutic discovery programs, a similar cassette dosing method can be easily applied for the measurement of brain:plasma distribution partition coefficients (K_p) via sampling of brain and blood at a single time point from one animal or at several time points from multiple animals (i.e., nonserial sampling) (Liu et al. 2012). Unbound brain:unbound plasma K_p values ($K_{p,uu}$) calculated using fraction unbound (f_u) from in vitro plasma protein and brain homogenate binding (PPB and BHB, respectively) assays can be obtained to identify compounds exhibiting rapid, unrestricted equilibrium of unbound compound in plasma with that in brain (i.e., $K_{p,uu}$ ~0.5–2) (Kalvass et al. 2007; Liu et al. 2008). For compounds possessing $K_{p,uu}$ values that are exceptionally low (i.e., <0.5) or high (i.e., >2), a subsequent investigation of their membrane permeability characteristics and/or propensity for active transport using common in vitro cellular approaches (e.g., bidirectional MDCK-MDR1; Pgp) can be used to determine the underlying mechanism(s) involved, subsequently serving to inform medicinal chemistry optimization strategies.

Through the integration and modification of these methods, we've designed and implemented an efficient approach to simultaneously define the plasma PK and brain tissue distribution (BTD) profiles of small molecule test compounds using low volumes of DMSO stock solutions, reduced animal census, and efficient use of LC/MS/MS bioanalytical resources. Herein, we describe the details and utility of this approach exemplified by its application towards the identification of allosteric modulator drug candidates targeting a CNS-expressed 7TM receptor.

Materials and Methods

Reagents

Solvents or reagents were of the highest purity commercially available and purchased from Sigma-Aldrich (St. Louis, MO) unless otherwise stated. Rat (male, SD) hepatic microsomes were obtained from BD Biosciences (Woburn, MA). Rat (male, SD) plasma and whole brain tissue were obtained from Bioreclamation (Westbury, NY). Minimum essential medium (MEM), phosphate-buffered saline (PBS) and Hank's Balanced Salt Solution (HBSS) were obtained from VWR International (Radnor, PA). Corning plastic tubes, serological pipettes, T-25 and T-75 flasks, and BD Falcon™ cell culture inserts (transparent PET membrane, 0.4 μmol L^{-1} pore size and 0.33 cm^2 surface areas), 24-well insert companion plates, Thermo Scientific Hyclone™ fetal bovine serum (FBS) were purchased from Fisher Scientific (Waltham, MA). Versene (0.48 mmol L^{-1}, with EDTA, in PBS) was obtained from Life Technologies (Carlsbad, CA). Small molecule test articles utilized in the present studies were prepared and characterized (identity/purity) in the Medicinal Chemistry Laboratory of the Vanderbilt Center for Neuroscience Drug Discovery (Nashville, TN).

Plasma protein binding, brain homogenate binding, and intrinsic clearance

The plasma protein and nonspecific brain homogenate binding of each compound, as well as intrinsic clearance (CL_{int}) was determined in plasma or brain homogenate using equilibrium dialysis as previously described (Bridges et al. 2013) and the half-life approach in hepatic microsomes (Obach 1999), respectively; additional details and relationships of f_u in plasma ($f_{u,plasma}$) and f_u in brain homogenate ($f_{u,brain}$) are provided in the Data S1.

Permeability and bidirectional efflux assessment

The culturing and execution of transwell-plate membrane assays employing MDCK cell methodology was performed as described in the Data S1.

Pharmacokinetics and brain tissue distribution studies in sprague–dawley rats

A cassette of compounds (n = 5/cassette) were formulated from 10 mmol L^{-1} solutions prepared in DMSO. In order to reduce the absolute volume of DMSO that was administered, the compounds were combined and diluted with ethanol and PEG 400 to achieve a final concentration of 0.4 mg mL^{-1} for each compound (2 mg mL^{-1} total) administered in each cassette; the maximal dosing volume was 0.5 mL kg^{-1} of each animal's body mass. The final dosing solutions consisted of approximately 10% ethanol, 40% PEG400, and 50% DMSO (v/v). Each cassette dose was administered IV via the jugular vein to one dual-cannulated (carotid artery and jugular vein) adult male Sprague–Dawley rat, each weighing between 250 and 350 g (Harlan, Indianapolis, IN) for a final dose of 0.2 mg kg^{-1} per compound. Whole blood collections via the carotid artery were performed at 0.033, 0.117, 0.25, 0.5, 1, 2, 4, 7, and 24 h post dose. The samples for PK analysis were collected into chilled, EDTA-fortified tubes and centrifuged for 10 min (1700 g, 4°C), with the resulting separated plasma stored at −80°C until LC/MS/MS bioanalysis. After re-administration of the cassette dose (i.e., dose number two), the samples for BTD analysis were collected at the time of euthanization (0.25 h post-re-administration), with the whole brain being removed and thoroughly rinsed with cold phosphate-buffered saline prior to freezing on dry ice. Whole brains were weighed and diluted (3 mL) with 70:30 isopropanol: water (v/v). The mixture was subjected to mechanical homogenation employing a Mini-Beadbeater™ and 1.0 mm Zirconia/Silica Beads (BioSpec Products Inc., Bartlesville, OK) followed by centrifugation (3500 g, 20°C, 5 min). The liquid extraction of plasma (40 μL) and brain homogenate supernatant diluted (4X) in plasma (40 μL) was performed by conventional protein precipitation using three volumes of ice-cold acetonitrile containing an internal standard (50 nmol L^{-1} carbamazepine). The samples were centrifuged (3500 g, 20°C, 5 min) and the supernatants diluted (1:1; v/v) via transfer into a fresh 96-well plate containing HPLC grade water. A detailed description of the LC/MS/MS bioanalysis of plasma and brain tissue is provided in the Data S1 and as previously described (Bridges et al. 2013).

Results and Discussion

A rapid pharmacokinetics and brain tissue distribution study design in sprague–dawley rat

During the lead optimization of small molecule allosteric modulators of a central 7TM receptor, we assessed the in vivo PKs and BTD of 70 novel compounds employing a combination PK and BTD study design utilizing IV cassette dosing (4 compounds plus 1 reference compound per study, 14 studies total; Fig. 1) in one rat per study. Compounds were selected for inclusion into the rapid PK-BTD studies based on in vitro pharmacological potency and receptor selectivity, as well as to explore PK and CNS penetration (i.e., $K_{p,uu}$) SAR across multiple chemical series. The compounds' molecular weights spanned a relatively narrow range (313.4–467.5 Da; mean 394.1 Da) while calculated log octanol:water partition coefficient (cLogP) values were more varied (−0.32–5.13; mean 1.82) as were other physicochemical properties (e.g., topological polar surface area, # rotatable bonds, etc.; data not shown), thus reflecting the diverse structural content of the compound set investigated. For each cassette study, plasma samples as well as brain samples diluted in plasma were jointly analyzed by a single LC/MS/MS method and quantitated using a single cassette-standard-curve prepared by combining predetermined quantities of each analyte into one set of plasma samples containing all standards (Fig. 1).

Hepatic microsomal CL_{int} as well as $f_{u,plasma}$ were obtained for all compounds subjected to the rapid PK-BTD cassette studies (Table 1). Both of these in vitro parameters varied widely across the compounds investigated. In vitro CL_{int} data are often critical to establishing the structure-metabolism-activity relationships within a chemical series (Balani et al. 2005), thus providing the medicinal chemist with insight to compounds' propensity for oxidative biotransformation, as well as providing a means to derive a predicted hepatic clearance (CL_{hep}) (Obach 1999). For compounds cleared principally by hepatic P450-mediated metabolism, CL_{hep} values predicted from microsomal CL_{int} data using the well-stirred model of organ clearance, uncorrected for f_u in microsomes ($f_{u,mics}$) and excluding the $f_{u,plasma}$ term, will serve as an upper limit for in vivo CL_p (i.e., predicted $CL_{hep} \geq CL_p$) with the exception of generally rare cases involving compounds possessing far lower $f_{u,mics}$ than $f_{u,plasma}$. Therefore, in conjunction with CL_p from the PK-BTD cassette studies, CL_{hep} prediction via the described approach provided a measure of in vitro to in vivo correlation (IVIVC) for all compounds investigated; not surprisingly, in the case of highly plasma protein bound

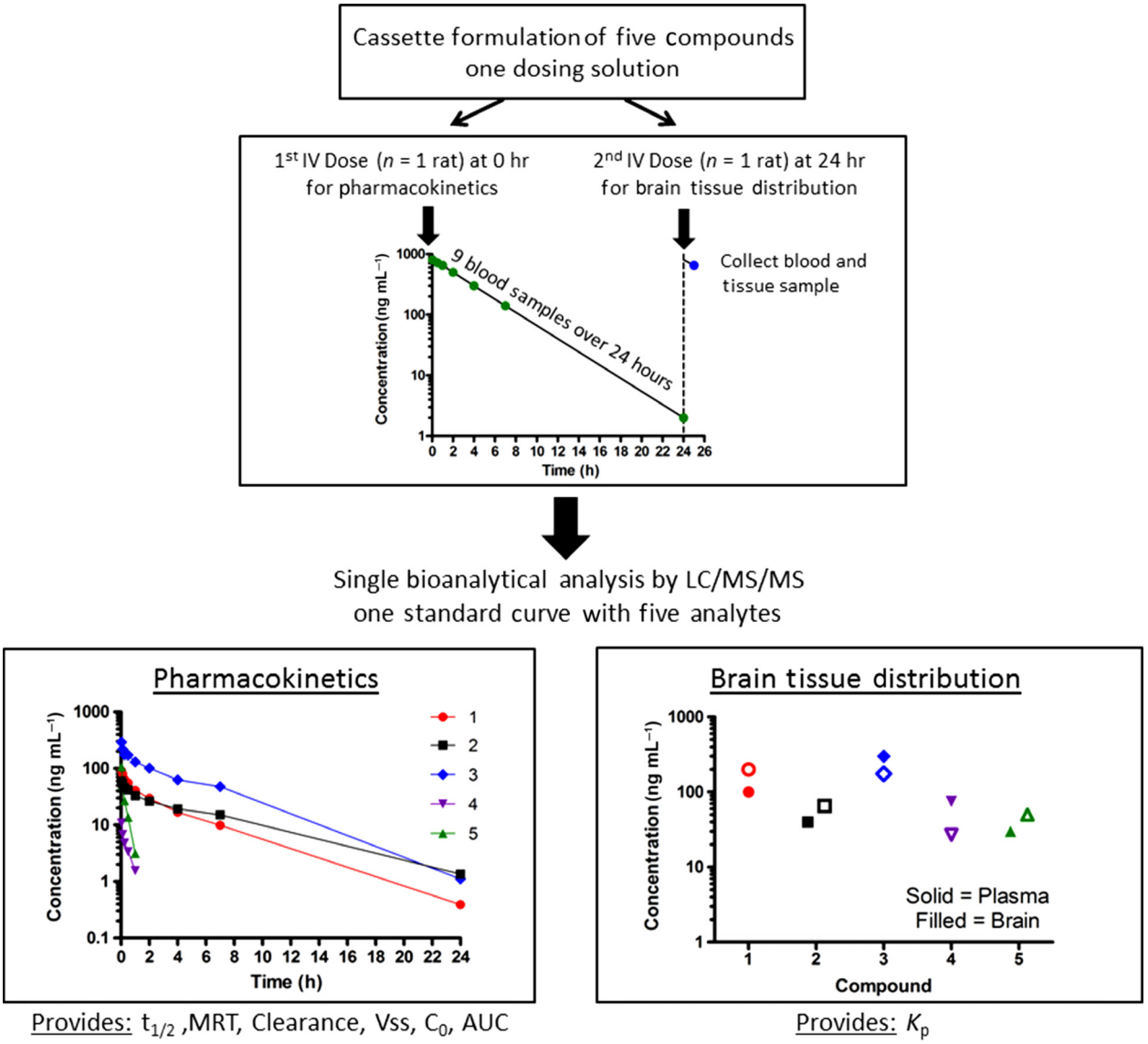

Figure 1. Combined pharmacokinetic (PK) and brain tissue distribution (BTD) IV cassette study paradigm. Formulation of a single cassette dosing solution containing five compounds is administered to one rat with serial blood collection over 24 h (PK data) followed by a redose of the same cassette of compounds with 0.25 h sampling of brain and blood (BTD data). Samples are analyzed by LC/MS/MS and all analytes quantitated from a single 'cassette standard curve' containing known amounts of each compound.

compounds (e.g., $f_{u,plasma} \ll 0.01$) that displayed moderate to high predicted CL_{int}, the in vivo CL_p was much lower than predicted CL_{hep} (e.g., compound 1).

Bioanalysis of brain tissue and plasma from a single time-point (0.25 h post administration) provided CNS K_p for all compounds (Table 1), which also varied widely. And while brain concentration data obtained over an entire time course (and the resulting AUC) is useful for a more clear definition of CNS distribution and kinetics, these data may be obtained subsequent to the advancement of a given compound of interest through a cross-functional project team's testing paradigm and after other key in vitro and/or in vivo compound characteristics have been determined (e.g., drug–drug interaction liabilities, reactive metabolism, behavioural or pharmacodynamic efficacy, ancillary pharmacology, etc.) or when more advanced PK studies are executed (Balani et al. 2005). Thus, the single time-point (0.25 h) BTD data obtained in our studies facilitated the rapid identification of compounds and structural series exhibiting an appreciable degree of brain penetration (i.e., $K_p > 0.05$) well in advance of a typical conventional assessment (Zhang et al. 2004).

Table 1. In vitro properties and rat PK-BTD IV cassette study results.

Compound	CL_{int}	Pred. CL_{hep}	CL_p	$f_{u,plasma}$	$f_{u,brain}$	B:P K_p	B:P $K_{p,uu}$
1	134	46	1.62	0.002	0.020	0.11	1.10
2	2.70	2.60	11.3	0.177	0.626	<0.05	<0.18
3	24.7	18.2	221	0.140	0.112	3.36	2.69
4	38.3	24.8	14.5	0.072	0.136	<0.10	<0.10
5	51.9	29.8	60.7	0.046	0.148	0.15	0.48
6	60.8	32.5	4.60	0.029	0.159	<0.10	<0.12
7	154	48.1	40.5	0.050	0.051	1.06	1.08
8	33.2	22.5	31.1	0.100	0.211	0.50	1.06
9	155	48.2	127	0.005	0.047	0.32	3.01
10	95.9	40.5	12.3	0.004	0.003	1.03	0.77
11	65.5	33.8	76.5	0.372	0.334	<0.24	<0.22
12	51.1	29.5	3.20	0.040	0.150	0.13	0.49
13	9.31	8.22	644	0.455	–	<1.51	–
14	42.4	26.4	80.9	0.259	0.322	<0.11	<0.13
15	<1.00	<1.00	284	0.509	–	<4.62	–
16	62.6	33.1	6.01	0.020	0.060	0.02	0.06
17	74.1	36.0	7.54	0.018	0.031	0.11	0.19
18	72.6	35.6	44.0	0.028	0.028	<0.16	<0.16
19	24.1	17.9	18.3	0.110	–	0.16	–
20	77.4	36.8	41.3	0.105	–	0.42	–
21	95.1	40.3	48.7	0.177	–	0.29	–
22	101	41.4	25.1	0.106	–	0.25	–
23	14.5	12.0	6.39	0.110	–	0.58	–
24	28.1	20.1	18.0	0.079	–	3.95	–
25	134	46.0	1.55	0.002	0.020	0.11	1.10
26	81.6	37.7	1.74	0.004	–	0.14	–
27	57.1	31.5	3.50	0.002	–	0.22	–
28	145	47.2	4.39	0.007	0.113	0.02	0.32
29	106	42.1	37.0	0.067	–	<0.20	–
30	204	52.1	22.8	0.047	0.166	<0.37	<1.31
31	45.8	27.7	0.99	0.109	0.015	0.05	0.01
32	55.0	30.8	–	0.457	–	–	–
33	132	45.7	70.2	0.144	–	<0.16	–
34	67.2	34.3	3.34	0.008	–	0.08	–
35	20.1	15.6	3.46	0.026	0.115	0.03	0.13
36	80.5	37.5	2120	0.515	–	<6.62	–
37	192	51.3	36.2	0.043	–	<0.64	–
38	88.3	39.0	21.9	0.104	–	0.06	–
39	29.5	20.8	1.32	0.077	0.054	0.03	0.02
40	162	48.9	14.6	0.019	0.051	0.23	0.62
41	86.1	38.6	12.1	0.043	–	<1.78	–
42	58.5	31.9	3.26	0.014	–	<0.85	–
43	24.1	17.9	8.76	0.014	0.038	0.12	0.33
44	71.2	35.3	3.46	0.007	–	0.06	–
45	71.2	35.3	8.92	0.017	0.002	0.33	0.04
46	239	54.1	13.8	0.016	–	0.07	–
47	26.5	19.2	4.94	0.023	–	0.03	–
48	20.4	15.8	3.55	0.026	–	0.03	–
49	24.8	18.3	13.9	0.030	0.032	0.14	0.15
50	119	44.1	5.17	0.019	–	0.06	–
51	59.5	32.2	16.5	0.021	–	0.08	–
52	146	47.3	19.1	0.017	–	0.05	–
53	98.2	40.9	10.6	0.012	–	0.10	–
54	118	43.9	115	0.059	–	0.13	–
55	26.7	19.3	5.66	0.012	–	0.06	–

(*Continued*)

Table 1. Continued.

Compound	CL_{int}	Pred. CL_{hep}	CL_p	$f_{u,plasma}$	$f_{u,brain}$	B:P K_p	B:P $K_{p,uu}$
56	9.30	8.21	3.46	0.014	–	0.10	–
57	19.5	15.2	2.08	0.017	–	0.06	–
58	48.7	28.7	3.72	0.019	–	0.12	–
59	860	64.7	44.0	0.048	–	<0.07	–
60	44.1	27.0	5.42	0.007	0.036	0.23	1.18
61	65.4	33.8	9.72	0.015	–	0.06	–
62	38.7	24.9	1.03	0.007	–	0.05	–
63	60.5	32.4	2.09	0.014	–	0.07	–
64	42.7	26.5	10.8	0.011	0.070	0.12	0.76
65	24.0	17.9	1.16	0.027	–	0.03	–
66	32.5	22.2	2.90	0.020	–	0.04	–
67	13.0	11.0	3.22	0.029	–	0.11	–
68	43.5	26.8	3.32	0.017	–	0.04	–
69	790	64.3	20.5	0.013	–	0.22	–
70	15.8	12.9	5.63	0.045	–	<0.20	–

CL_{int}, intrinsic clearance; CL_{hep}, predicted hepatic clearance; CL_p, plasma clearance (noncompartmental analysis); $f_{u,plasma}$ and $f_{u,brain}$, unbound plasma and brain, respectively; K_p, brain partition coefficient; $K_{p,uu}$, unbound brain:unbound plasma partition coefficient; -, not determined.

Based on these compounds' respective pharmacological activity and their cassette PK profiles, $f_{u,brain}$ was then determined by a BHB assay (via equilibrium dialysis; Table 1); specifically, this comprised a subset of 28 compounds of interest. For each of these compounds, the K_p values reflecting total concentrations were divided by fu_{plasma}/fu_{brain} in order to calculate respective $K_{p,uu}$, values representing unbound brain:unbound plasma concentrations (Table 1). As only unbound drug is available to bind the target protein and to equilibrate between plasma and extravascular tissues, determination and use of $K_{p,uu}$ in CNS drug discovery optimization programs represents the favoured approach for the understanding of compounds' brain distribution characteristics (desirable values for $K_{p,uu}$ near unity [~1]) (Kalvass et al. 2007; Liu et al. 2008; Friden et al. 2010). For freely permeable compounds that are not subject to active transport at the BBB, total concentrations in plasma and brain primarily reflect tissue-specific binding parameters (i.e., brain:plasma $K_p \sim [fu_{plasma}/fu_{brain}]$); therefore, K_p values alone should not be used to rank-order compounds or establish SAR, with the exception of cases involving compounds with exceptionally low K_p (e.g., <0.05) that are unlikely to penetrate the BBB. Furthermore, the 0.25 h BTD sampling time point chosen for use in the present paradigm is sufficient to capture detectable brain concentrations (even for low K_p compounds) and provide total and unbound brain:plasma partition coefficients. For very slowly equilibrating compounds whose 0.25 h BTD data might underestimate true K_p (and thus $K_{p,uu}$) in comparison to those derived from AUC-based data, these hypothetical false negatives can be tolerated as such compounds are typically to be avoided to begin with due to suboptimal physicochemical properties that would otherwise limit their utility as an orally bioavailable therapeutic drug candidate. Properties such as topological polar surface area (tPSA), log octanol-water partition coefficient (logP), and others such as number of rotatable bonds and molecular weight have been found to impact the rate and extent of transcellular permeation of the blood-brain barrier (BBB) due to their influence on intrinsic membrane permeability. Generally, compounds possessing low tPSA (e.g., <70 A^2), moderate logP (e.g., 2–4), few rotatable bonds (e.g., <8), and low molecular weight (e.g., <450) exhibit greater membrane permeability and hence passively diffuse across the BBB and reach equilibrium more rapidly than compounds bearing less optimal values for these properties, in the absence of active transport phenomena. Thus, late or slowly equilibrating compounds could be erroneously passed over if their brain:plasma K_p at the 0.25 h time point (in the cassette study) appears very low; ultimately, this is an acceptable tradeoff given the overall advantages of the approach and with the consideration that such compounds are likely to suffer from other issues rendering them less useful for advancement. As with other compound properties, the present studies revealed a wide range of $K_{p,uu}$ for these 7TM receptor modulators, the finding of which also provided exceptional value as to the identification of the structural attributes conducive to CNS distribution.

Correlation between cassette and discrete PK-BTD data obtained in rat

In order to determine the accuracy of the present approach, the PK and BTD profiles of compounds **1** and

2 (Table 1) were obtained from cassette studies and subsequently compared with those profiles originating from discrete studies; both compounds exhibited low CL_p in cassette studies, dissimilar brain:plasma $K_{p,uu}$ values, and substantially different values for $f_{u,plasma}$ and $f_{u,brain}$, respectively. Both compounds were examined in discrete PK studies (IV, 1 mg kg^{-1}, $n \geq 2$, non-DMSO vehicle) and discrete BTD studies (intraperitoneal [IP] or oral [PO], 10 mg kg^{-1}, $n \geq 2$, non-DMSO vehicle), which revealed parameters highly similar to those obtained from cassette PK-BTD studies (Fig. 2). Additionally, compound **1** was re-examined to determine the reproducibility of PK across multiple cassettes (Fig. 2, each replicate plotted individually, $n = 2$); indeed, we observed limited variability between studies with excellent agreement of concentration–time data and resulting PK parameters corresponding to each. Additionally, CL_p values from studies utilizing concurrent IV administration of low doses (0.2 mg kg^{-1}) of multiple compounds ($n = 5$ per study) from other structurally and pharmacological distinct scaffolds via cassettes formulated directly from DMSO stock solutions (10 mmol L^{-1}) were compared to those from discrete assessments in which a single compound was administered to multiple animals at a higher dose (1.0 mg kg^{-1}, typically prepared from solid material). A similar fidelity in PK results was observed across multiple cassette studies from these series of structurally diverse compounds (Table 2, Fig. 3). Furthermore, CL_p, V_{ss}, $t_{1/2}$, and K_p values for the reference compound used across most of the cassette studies exhibited low variability (Table S1). Thus, use of the combined PK-BTD cassette study design provides a substantial gain in efficiency without compromising data accuracy or reproducibility.

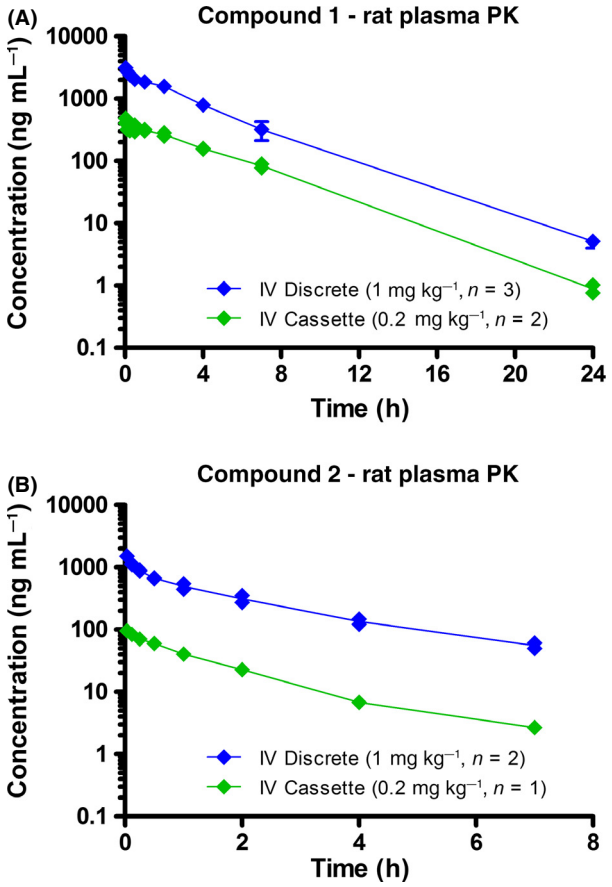

Figure 2. Pharmacokinetic (PK) and brain tissue distribution (BTD) time-concentration profiles of compounds 1 (A) and 2 (B) obtained from cassette (green) and discrete (blue) dosing in male, Sprague–Dawley rats.

Table 2. Plasma clearance (CL_p) values from cassette versus discrete rat IV PK studies.

Compound	CL_p (mL min^{-1} kg^{-1})	
	Cassette[1]	Discrete[2]
A	9.75	10.4
B	7.00	8.06
C	2.00	1.62
D	3.00	9.70
E	3.00	4.30
F	23.0	14.0
G	26.0	11.0
H	11.0	18.0
I	36.0	38.0
J	13.8	12.8

[1]0.2–0.25 mg kg^{-1} intravenous dose to male, SD rat ($n = 1$).
[2]1.0 mg kg^{-1} intravenous dose to male, SD rat ($n \geq 2$).

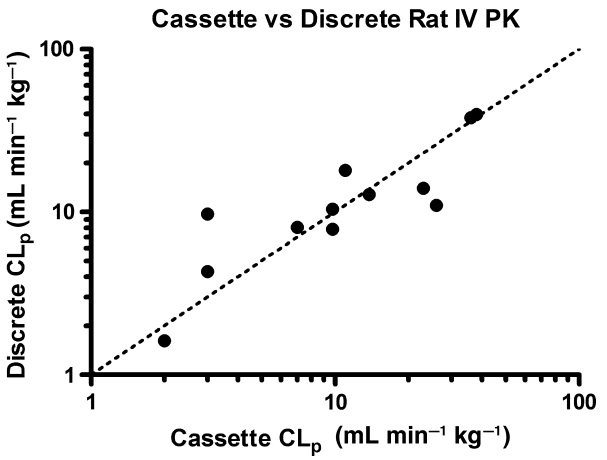

Figure 3. Plasma clearance (CL_p) values for ten additional compounds from distinct structural series obtained via pharmacokinetic (PK) studies employing either cassette ($n = 1$ animal) or discrete ($n \geq 3$ animals) assessments in male, Sprague–Dawley rat. Dotted line represents unity. Values from compounds 1 and 2 (Fig. 2) are also included.

Investigation of mechanism(s) contributing to low brain:plasma $K_{p,uu}$

Compounds that exhibited limited CNS exposure in vivo ($K_{p,uu}$ values approximately <0.5) were subjected to bidirectional permeability assessment (P_{app}) in MDCK cells (WT and MDR1-transfected) employing transwell membrane assay methodology (Xia et al. 2007); the assessment yielded pertinent efflux ratios (ER) which were framed against the in vivo $K_{p,uu}$ values. The results of these assays and related $K_{p,uu}$ values from the PK-BTD cassette studies are provided in Table 3. Likewise, a second set of compounds (Table 3) demonstrating $K_{p,uu} > 0.5$ were also examined for direct comparison to the more peripherally-restricted compound set. In general, compounds exhibiting lower $K_{p,uu}$ values possessed an ER suggestive of Pgp activity and/or a low P_{app}; several compounds did not fall into this generalization. For instance, compound **25** exhibited a $K_{p,uu}$ near unity despite having poor permeability and a higher ER than compound **28**, which exhibited similarly poor permeability (but an approximately threefold lower $K_{p,uu}$). Importantly, BBB-expressed efflux transporters (Xia et al. 2007) other than Pgp could be involved in such cases (e.g., **28**), or the contribution of an uptake transporter could be responsible for the favourable $K_{p,uu}$ of poorly permeable compounds (e.g., **25**). By deriving $K_{p,uu}$ from in vivo cassette BTD data prior to in vitro permeability or efflux transporter assessment, favourable compounds can be quickly identified in absence of specific knowledge of underlying mechanism (s); when available, mechanistic data can inform medicinal chemistry optimization efforts.

Table 3. Apparent permeability and Pgp efflux ratios for select compounds.

Compound	Brain-plasma $K_{p,uu}$	MDCK-WT P_{app} ($\times 10^{-6}$ cm/sec)	MDCK-Pgp efflux ratio
2	<0.18	6.5	11
31	0.01	4.9	8.9
45	0.04	2.3	2.3
35	0.13	24	2.2
49	0.15	30	1.9
28	0.32	4.6	0.8
43	0.33	6.4	8.5
40	0.62	8.8	2.4
10	0.77	42	n.d.
8	1.06	29	n.d.
7	1.08	27	n.d.
25	1.10	3.0	1.7
3	2.69	7.7	n.d.
9	3.01	22	n.d.

$K_{p,uu}$, unbound plasma:unbound brain partition coefficient; P_{App}, apparent permeability. n.d., not determined.

Application of the rapid PK-BTD study design

The novel IV cassette study design described herein facilitated rapid determination of both PK and BTD profiles for seventy compounds of interest while using less than twenty animals (total). Plasma clearance data were used to prioritize chemical series (or sub-series) possessing acceptable in vitro:in vivo correlation (IVIVC; $CL_p \leq CL_{hep}$) and to quickly eliminate those compounds displaying elevated clearance. The derivation of K_p and $K_{p,uu}$ values served to establish critical SAR predictive of CNS penetration within a chemical series, resulting in the progression of select compounds through the in vivo pharmacological testing paradigm for the therapeutic area (related to the 7TM receptor). Importantly, the conventional cassette-dosing approaches to determining rodent PK and BTD in early discovery programs are laborious and require higher rodent census ($n \geq 3$ animals) and non-serial sampling in order to obtain brain (and/or cerebrospinal fluid) AUC data in addition to that of plasma. Two dozen animals per compound is a typical census required for such studies and often necessitates intense bioanalytical resources for sample preparation and quantitation of compound(s) in multiple matrices. In contrast, the present paradigm leverages a more efficient approach, providing equivalent data value to a cross-functional discovery team at a fraction of the time and resources. However, it is important to note that application of this strategy is best suited to hit-to-lead and early lead-optimization where rapid assessment of PK and BTD of large numbers of compounds can be used as a means to rank order or 'bucket' compounds/subseries (e.g., 'low CL_p with poor CNS distribution') as opposed to serving as a means for definitive assessment of a lead compound's disposition, as the latter should only be obtained via discrete studies utilizing multiple animals in order to maximize accuracy.

It is also particularly noteworthy that the rapid PK-BTD study design is not limited to the CNS therapeutic area, but should be recognized as a paradigm that's adaptable to investigating distribution (i.e., K_p) to tissues other than the brain. For example, whole liver and lung can be rapidly assessed employing this study design and analyzed in conjunction with in vitro $f_{u,tissue}$ values for the determination of tissue:plasma $K_{p,uu}$. Together with the standard in vitro assay methodology used to obtain CL_{int} and $f_{u,plasma}$ (so-called Tier-1 screening), and with data from membrane permeability and/or active transport, the present approach may serve a universally applicable, integral component of resource-sensitive contemporary drug discovery organizations.

Disclosures

None declared.

References

Balani SK, Miwa GT, Gan LS, Wu JT, Lee FW (2005). Strategy of utilizing in vitro and in vivo ADME tools for lead optimization and drug candidate selection. Curr Top Med Chem 5: 1033–1038.

Bridges TM, Rook JM, Noetzel MJ, Morrison RD, Zhou Y, Gogliotti RD, et al. (2013). Biotransformation of a novel positive allosteric modulator of metabotropic glutamate receptor subtype 5 contributes to seizure-like adverse events in rats involving a receptor agonism-dependent mechanism. Drug Metab Dispos 41: 1703–1714.

Bueters T, Dahlstrom J, Kvalvagnaes K, Betner I, Briem S (2011). High-throughput analysis of standardized pharmacokinetic studies in the rat using sample pooling and UPLC-MS/MS. J Pharm Biomed Anal 55: 1120–1126.

Chen S, Wu JT, Huang R (2012). Evaluation of surrogate matrices for standard curve preparation in tissue bioanalysis. Bioanalysis 4: 2579–2587.

Christ DD (2001). Cassette dosing pharmacokinetics: valuable tool or flawed science? Drug Metab Dispos 29: 935.

Friden M, Ljungqvist H, Middleton B, Bredberg U, Hammarlund-Udenaes M (2010). Improved measurement of drug exposure in the brain using drug-specific correction for residual blood. J Cereb Blood Flow Metab 30: 150–161.

Goteti K, Brassil PJ, Good SS, Garner CE (2008). Estimation of human drug clearance using multiexponential techniques. J Clin Pharmacol 48: 1226–1236.

Hosea NA, Collard WT, Cole S, Maurer TS, Fang RX, Jones H, et al. (2009). Prediction of human pharmacokinetics from preclinical information: comparative accuracy of quantitative prediction approaches. J Clin Pharmacol 49: 513–533.

Huang R, Qian M, Chen S, Lodenquai P, Zeng H, Wu J-T (2004). Effective strategies for the development of specific, sensitive and rapid multiple-component assays for cassette dosing pharmacokinetic screening. Int J Mass Spectrom 238: 131–137.

Kalvass JC, Maurer TS, Pollack GM (2007). Use of plasma and brain unbound fractions to assess the extent of brain distribution of 34 drugs: comparison of unbound concentration ratios to in vivo p-glycoprotein efflux ratios. Drug Metab Dispos 35: 660–666.

Liu X, Chen C, Smith BJ (2008). Progress in brain penetration evaluation in drug discovery and development. J Pharmacol Exp Ther 325: 349–356.

Liu X, Ding X, Deshmukh G, Liederer BM, Hop CE (2012). Use of the cassette-dosing approach to assess brain penetration in drug discovery. Drug Metab Dispos 40: 963–969.

Mahmood I, Balian JD (1996). Interspecies scaling: predicting clearance of drugs in humans. Three different approaches. Xenobiotica 26: 887–895.

Obach RS (1999). Prediction of human clearance of twenty-nine drugs from hepatic microsomal intrinsic clearance data: an examination of in vitro half-life approach and nonspecific binding to microsomes. Drug Metab Dispos 27: 1350–1359.

Sadagopan N, Pabst B, Cohen L (2005). Evaluation of online extraction/mass spectrometry for in vivo cassette analysis. J Chromatogr B Analyt Technol Biomed Life Sci 820: 59–67.

Smith NF, Raynaud FI, Workman P (2007). The application of cassette dosing for pharmacokinetic screening in small-molecule cancer drug discovery. Mol Cancer Ther 6: 428–440.

White RE, Manitpisitkul P (2001). Pharmacokinetic theory of cassette dosing in drug discovery screening. Drug Metab Dispos 29: 957–966.

Xia CQ, Milton MN, Gan LS (2007). Evaluation of drug-transporter interactions using in vitro and in vivo models. Curr Drug Metab 8: 341–363.

Zhang MY, Kerns E, McConnell O, Sonnenberg-Reines J, Zaleska MM, Steven Jacobsen J, et al. (2004). Brain and plasma exposure profiling in early drug discovery using cassette administration and fast liquid chromatography-tandem mass spectrometry. J Pharm Biomed Anal 34: 359–368.

Supporting Information

Additional Supporting Information may be found in the online version of this article:

Data S1. Detailed protocol and additional information for the MDCK-WT permeability and MDCK-MDR1 transport assays.

Table S1. Mean values and standard deviations for PK and BTD parameters of a reference compound used in combination cassette studies (n = 14).